Biomedicine & Pharmacotherapy 150 (2022) 112996

Contents lists available at ScienceDirect

Biomedicine & Pharmacotherapy

journal homepage: www.elsevier.com/locate/biopha

CXCL12 inhibits hair growth through CXCR4

Mei Zheng [a,1], Sang Ho Oh [b,1], Nahyun Choi [a], Yong Jin Choi [a], Jino Kim [c], Jong-Hyuk Sung [a,d,*]

[a] Epi Biotech Co., Ltd., Incheon 21983, South Korea
[b] Department of Dermatology and Cutaneous Biology Research Institute, Severance Hospital, Yonsei University College of Medicine, Seoul 03722, South Korea
[c] New Hair Institute, Seoul 06134, South Korea
[d] College of Pharmacy, Institute of Pharmaceutical Sciences, Yonsei University, Incheon 21983, South Korea

ARTICLE INFO

Keywords:
Dermal fibroblast
Hair loss
Hair follicle
CXCL12
CXCR4

ABSTRACT

CXCL12 and its receptors, which are highly expressed in the skin, are associated with various cutaneous diseases, including androgenic alopecia. However, their expression and role during the hair cycle are unknown. This study aims to investigate the expression of CXCL12 and its receptor, CXCR4, in the vicinity of hair follicles and their effect on hair growth. CXCL12 was highly expressed in dermal fibroblasts (DFs) and its level was elevated throughout the catagen and telogen phases of the hair cycle. CXCR4 is expressed in the dermal papilla (DP) and outer root sheath (ORS). In hair organ culture, hair loss was induced by recombinant CXCL12 therapy, which delayed the telogen-to-anagen transition and decreased hair length. In contrast, the suppression of CXCL12 using a neutralizing antibody and siRNA triggered the telogen-to-anagen transition and increased hair length in hair organ culture. Neutralization of CXCR7, one of the two receptors for CXCL12, only slightly affected hair growth. However, inhibition of CXCR4, the other receptor for CXCL12, increased hair growth to a considerable extent. In addition, in hair organ culture, the conditioned medium from DFs with CXCL12 siRNA considerably increased the hair length and induced proliferation of DP and ORS cells. CXCL12, through CXCR4 activation, increased STAT3 and STAT5 phosphorylation in DP and ORS cells. In contrast, blocking CXCL12 and CXCR4 decreased the phosphorylation of STAT3 and STAT5. In summary, these findings suggest that CXCL12 inhibits hair growth via the CXCR4/STAT signaling pathway and that CXCL12/CXCR4 pathway inhibitors are a promising treatment option for hair growth.

1. Introduction

C-X-C motif chemokine 12 (CXCL12), also known as stromal cell-derived factor 1 (SDF1), is a small cytokine member of the chemokine family. Chemokines activate leukocytes and are frequently generated by pro-inflammatory stimuli such as lipopolysaccharide, tumor necrosis factor, and interleukin 1 [1–3]. CXCL12 is found expressed in various mouse tissues, including the brain, thymus, heart, lung, liver, kidney, spleen, and bone marrow [4]. It regulates the migration of hematopoietic cells from the fetal liver to the bone marrow as well as the formation of large blood vessels during embryogenesis [5]. It has been assumed that CXCL12 only binds to one receptor, C-X-C motif chemokine receptor 4 (CXCR4), but recent research has shown that CXCL12 may also bind to CXCR7 receptor [6,7]. Because of its role in morphogenesis, angiogenesis, and immune responses, CXCL12 and its receptors are prospective targets for drug development [8,9]. CXCL12 contributes significantly to angiogenesis during adulthood by attracting bone marrow-derived endothelial progenitor cells via a CXCR4 dependent pathway [10]. The CXCL12-CXCR4 axis is being studied as a potential antifibrotic therapy for chronic pancreatitis [11]. Additionally, in a xenograft model of breast cancer and hepatocellular carcinoma, plerixafor (AMD3100) blocks CXCL12from binding CXCR4, increasing the efficacy of combretastatin [12,13]. AMD3100 is commonly combined with granulocyte colony-stimulating factor (G-CSF) to mobilize hematopoietic stem cells into the bloodstream [14–16]. Moreover, CXCL12 and its receptor CXCR4 regulate melanoblast migration and location during the hair

Abbreviations: DPCs, dermal papilla cells; ORS, outer root sheath cells; DFs, dermal fibroblast cells; HFs, hair follicles; CXCL12, C-X-C Motif Chemokine Ligand 12; αCXCL12, anti-CXCL12 neutralizing antibody; rCXCL12, recombinant mouse CXCL12; AA, alopecia areata; STAT, signal transducer and activator of transcription; ALP1, alkaline phosphatase 1.

* Correspondence to: College of Pharmacy, Yonsei University, 85 Songdogwahakro, Yeonsu-gu, Incheon 21983, South Korea.
E-mail addresses: brian99@yonsei.ac.kr, brian99@empal.com (J.-H. Sung).

[1] Equal contribution

https://doi.org/10.1016/j.biopha.2022.112996
Received 13 February 2022; Received in revised form 12 April 2022; Accepted 17 April 2022
Available online 21 April 2022

follicle (HF) formation and cycle [17]. Additionally, Lee et al. found that CXCL12 and its receptor CXCR7 control the migration of normal human epidermal melanocytes [18]. However, there is no direct evidence that CXCL12 regulates hair growth and cycle.

Interestingly, Michel et al. identified differential gene expression in male androgenetic alopecia (AGA). They hypothesized that inflammatory and immunological mediators were considerably overexpressed, with significant upregulation of immune and inflammatory genes, including *CCL13*, *CCL18*, *CXCL10* and *CXCL12* [19]. Given that CXCL12 has a very high baseline expression, we postulated that CXCL12 regulates the hair cycle and is involved in hair loss in AGA. In alopecia areata (AA), an autoimmune disease that induces hair loss, human dermal γδ T cells are known to act as stress sentinels by directly eliciting autoimmune reactions. In addition, in AA, stressed hair follicles overexpress the γδ T cell chemoattractants CXCL10 and CXCL12 [20,21]. These findings suggest that CXCL12 and CXCR4 may play a role in hair loss in various disorders and that blocking CXCL12/CXCR4 pathway may be a therapeutic target for hair loss [22]. However, the expression and role of CXCL12 and its receptor in normal hair cycle have not been elucidated yet. Therefore, we sought to identify where CXCL12 and CXCR4 are expressed in the skin and HF, how they are regulated by the hair cycle, and whether inhibiting CXCL12 and CXCR4 pathways stimulate hair growth. The underlying molecular mechanism and signaling pathway driving hair loss were also investigated.

2. Materials and methods

2.1. Cell isolation and cell culture

Individual HFs were kindly gifted by Dr. Jino Kim (New Hair Institute, South Korea). All biopsies were performed with full patient written consent. Additionally, the Ethical and Scientific Committees of the participating institution confirmed the present study to be in accordance with the ethical standards (as laid out in the 1964 Declaration of Helsinki).

Human follicle dermal papilla (hDP) cells, and outer root sheath (hORS) cells were microdissected from the HFs under a stereomicroscope. The lower part of the bulb was inverted using forceps and needles, and any remaining epithelium-derived tissue was removed to expose the dermal papilla, and then DP was attached to CellBIND® surface 35-mm culture dish (Corning, USA), attached hair shaft (outer root sheath; middle part of HF) to Collagen I coated 35-mm culture dish (Corning), and cultured undisturbed for ten days.

hDP cells were cultured in follicle dermal papilla cell growth medium (PromoCell, Germany) with 1% antibiotic-antimycotic (Thermo Fisher Scientific, USA). hORS cells were cultured in EpiLife™ Medium with 60 μM calcium chloride, 1% EpiLife™ Defined Growth Supplement (EDGS) (Thermo Fisher Scientific, USA), and 1% antibiotic-antimycotic (Thermo Fisher Scientific). Dermal fibroblast (DF) cells were kindly gifted by Prof. Sang Ho Oh (Severance Hospital, Yonsei University College of Medicine, Seoul, Korea) and cultured in Dulbecco's modified Eagle's medium (DMEM; Gibco, Germany) with 10% fetal bovine serum (FBS; Hyclone, USA), and maintained in a humidified incubator at 37 °C with 5% CO_2.

2.2. Animals

Male adult (4–7 weeks old) C3H/HeN mice were purchased from Orient Bio Co. Ltd (SungNam, Korea). All animal studies were conducted with the approval of the Animal Care and Use Committee at the International Medical Center to reduce suffering and protect animal welfare.

2.3. Proliferation assay

Cell proliferation was determined using a cell counting kit-8. hDP cells (passage 5) were plated overnight in triplicate in 96-well plates at 1000–1500 cells per well. hORS (passage 3) were plated overnight in triplicate in 48-well plates at 6000–7000 cells per well. After 24 h, the culture medium was replaced with DFCMcon-si or DFCMCXCL12-si for 48 h (Fig. 6). After incubation, the medium was replaced by CCK-8 solution (Dojindo, Kumamoto, Japan), followed by an incubation for 2 h. The absorbance was measured at 450 nm using a microplate reader (TECAN, AG, Switzerland).

2.4. Scratch migration assay

Cell migration was detected using a scratch migration assay. 5×10^5 ORS cells (passage 3) were seeded in 35-mm dishes with growth medium. The following day, the growth medium was replaced with basal medium. Confluent cells were wounded using a sterile 1 mL pipette tip and incubated in either $DFCM^{con\text{-}si}$ or $DFCM^{CXCL12\text{-}si}$. Cell migration was determined via microscopic examination 48 h after wounding. To evaluate of cell migration, three randomly selected points along each wound were marked, and horizontal distances of migrating cells from the wound edge were measured.

2.5. Reverse transcription-quantitative polymerase chain reaction (RT-qPCR) assay

Quantitative real-time PCR (qRT-PCR) reactions were performed using StepOne Real-Time PCR System (Applied Biosystems, USA). The total cellular RNA was extracted using Invitrogen TRIzol Reagent (Thermo Fisher Scientific), followed by reverse-transcription using a cDNA synthesis kit (Nanohelix, Daejeon, Korea.). Real-time quantitative reverse-transcription polymerase chain reaction (qRT-PCR) was performed using the StepOne Real-Time PCR System (Applied Biosystems/Thermo Fisher Scientific). The primer sequences that were used are as follows (forward and reverse, respectively: 5′-CGCCAAGAACCTCATCATCT-3′ and 5′-GTCTCGGTGGATCTCGTATTTC-3′ for human ALP1, 5′-TGCATCAGTGACGGTAAACCA-3′ and 5′-TTCTTCAGCCGTGCAACAATC-3′ for mouse Cxcl12, 5′- ATTCTCAACACTCCAAACTGTGC-3′ and 5′- ACTTTAGCTTCGGGTCAATGC-3′ for human CXCL12. 5′- AGCCTGGCAACTACTCTGACA-3′ and 5′- GAAGCACGTTCTTGTTAGGCA-3′ for mouse Cxcr7.

2.6. Immunofluorescence staining for paraffin sections

Mouse skin tissue slides were de-paraffinized and incubated with boiling antigen retrieval solution (pH 6.0; Dako, Carpinteria, CA, USA) using a microwave oven for 2 m 20 s. The slides were then washed with 0.05% triton in phosphate-buffered saline (PBS-T) and incubated with anti-CXCL12 (1:100, R&D systems, MAB350-SP), anti-PDGFRα (1:100, Bioss, Beijing, China, BSM-52829R), anti-p-STAT3 (1:100, Cell signaling Technology, USA, #9145T), anti-p-STAT5 (1:100, Cell signaling Technology, #4322T), anti-CXCR4 (1:100, Novus Biologicals, Colorado, United States, NB100–56437), anti-CXCR7 (1:100, Novus Biologicals, NBP2–58162), and keratin 17 (1:100, Santa Cruz, California, United States, sc-393002) overnight at 4 ℃. They were then incubated with Alexa Fluor 488 goat anti-mouse IgG (1:500; Invitrogen, Grand Island, NY, USA), Alexa Fluor 488 goat anti-rabbit IgG (1:500; Invitrogen), Alexa Fluor594 goat anti-rabbit IgG (1: 200; Invitrogen), or Alexa Fluor 594 goat anti-mouse IgG (1:200, Invitrogen) for 1 h at room temperature with 4′,6-diamidino-2-phenylindole (DAPI; Sigma-Aldrich, Louis, MO, United States). Images obtained via immunofluorescence staining were captured using a Zeiss LSM700 confocal microscope.

2.7. Immunofluorescence staining for cells

Fixed hDP and hORS cells were treated with primary antibodies specific for p-STAT3 or p-STAT5 (1: 200, Cell Signaling) at 4 ℃. On the following day, cells were washed with PBS-T and then incubated with Alexa Fluor 488 goat anti-rabbit IgG (1:500) for 1 h at room

temperature. Nuclei were counterstained using DAPI. Images of immunofluorescence staining were captured using a Zeiss LSM700 confocal microscope.

2.8. Hair organ culture

During organ culture, the hair growth activity of mouse vibrissae, and human HFs was observed. The hair growth activity of mouse vibrissae and adult scalp hair follicles was observed during organ culture. The HFs were isolated and cultured according to the method previously described by Jindo and Tsuboi [23]. Normal anagen vibrissal HFs and adult scalp HFs were obtained from the upper lip region using a scalpel and forceps. Isolated HFs were placed in a defined medium (Williams E medium supplemented with 2 mM L-glutamine, 10 μg/mL insulin, 10 ng/mL hydrocortisone, 100 U/mL penicillin, and 100 μg/mL streptomycin, without serum). Individual vibrissae HFs and adult scalp HFs were photographed 48–96 h after the start of the incubation. Changes in hair length were calculated from the photographs and expressed as mean ± SE of 10–12 vibrissae HFs or human scalp HF.

2.9. Telogen-to-anagen transition (anagen induction) and neutralizing antibodies

Animal experiments were performed according to Kim [24] and Paus et al. [25], pharmacopoeia and the Institutional Animal Care and Use Committee of Yonsei University (IACUC-A-202111-1380-01). The dorsal area (2.5 cm × 4 cm) of 6-week-old, 22–24 g C_3H/HeN mice, which were in the telogen stage of the hair cycle, were shaved using a clipper and electric shaver, with special care taken to avoid damaging the skin. Subcutaneous injection of recombinant protein, neutralizing antibodies, siRNA, or antagonist against CXCR4 was administered for 2 weeks. Any darkening of the skin (indicative of hair cycle induction) was carefully monitored via photography. After 2 weeks, dorsal hair was shaved and weighted. The number of anagen hair shafts was counted after hematoxylin and eosin (H & E) staining. The following neutralizing antibodies were used for *in vivo* study: αCXCL12, (R&D systems; MAB310–500), αCXCR4 (R&D systems; MAB21651), and αCXCR7 (US Biological, USA, C8376–25 L).

2.10. Anagen elongation

The anagen phase was induced by depilation on the dorsal skin of 7-week-old male mice. All depilated mouse HFs were synchronized in the telogen phase. After 10 days, the animals were topically treated with either control, αCXCL12, or rCXCL12 (PeproTech, USA) for 7 consecutive days. The dorsal skin of mice was observed, and photographs were captured 17 days after depilation. The number of anagen and catagen hair shafts was observed by H & E staining.

2.11. Knockdown of CXCL12 in vivo and ex vivo

CXCL12 expression was knocked down in 7-week-old C_3H mice by transfecting with 6 μg of CXCL12 siRNA (Bioneer, Daejeon, Korea) using the transfection reagent Polyplus *in vivo*-jetPEI (Polyplus-transfection, France, #201-50G). The primer sequences used were as follows, si-CXCL12-#a sense, 5′-GAACAACAACAGACAAGUG-3′ and anti-sense, 5′-CACUUGUCUGUUGUUGUUC-3′; si-CXCL12-#b sense, 5′- GUGGAUUCAGGAGUACCUG-3′ and anti-sense, 5′-CAGGUACUCCUGAAUCCAC-3′; si-CXCL12-#c sense, 5′- CAGACAAGUGUGCAUUGAC-3′ and anti-sense, 5′-GUCAAUGCACACUUGUCUG-3′; si-CXCL12-#d sense, 5′- AUUCUCAACACUCCAAACU-3′ and anti-sense, 5′-AGUUUGGAGUGUUGAGAAU-3′.

2.12. Knockdown of CXCL12 in vitro

Transfections were performed using Lipofectamine RNAimax reagent (Invitrogen, USA).

2.13. Measurement of CXCL12 by enzyme-linked immunosorbent assay (ELISA)

Media containing transfection agent and si-CXCL12 was removed and replaced with fresh media. After 48 h of culture, the conditioned medium was collected and centrifuged to remove debris. The CXCL12 content was measured by ELISA kits (R&D systems; #DSA00). ELISA was performed according to the manufacturer's instructions. All samples were measured three times.

2.14. Statistical analysis

All data are expressed as mean ± standard deviation of three independent experiments. Student's *t*-test was used when comparing between two groups and one-way ANOVA or two-way ANOVA with Tukey's post hoc test were used for comparing multiple groups. A $p < 0.05$ was considered statistically significant. All statistical analyses were conducted using GraphPad Prism 5.01 (GraphPad Software, Inc., La Jolla, CA, USA). Graph building was performed using Sigma Plot 10.0 (Systat Software, San Jose, California, United States).

3. Results

3.1. CXCL12 is highly expressed in DFs during catagen/telogen phase

Double immunostaining of CXCL12 with platelet-derived growth factor receptor α (PDGFRα), an indicator for DFs, was conducted to study the distribution of CXCL12 in mice during the hair cycle. PDGFRα-positive cells were used to normalize the percentage of CXCL12-positive cells in this analysis (Fig. 1A). Based on confocal images, CXCL12 was highly expressed in DFs and considerably more elevated in mice throughout the catagen/telogen phase. mRNA levels of CXCL12 were upregulated in mouse skin in the hair regression period (Fig. S1; see Supporting Information). Furthermore, the CXCL12 expression level was higher in the bald area of the aged mice (>18 months) than in the non-bald areas (Fig. 1B), indicating that CXCL12 is linked to hair loss.

3.2. Treatment of CXCL12 delays anagen entry, and induces catagen entry

The effect of CXCL12 on the hair cycle progression was evaluated using telogen phase C_3H mice. Mice injected subcutaneously with 0.4 and 1.2 μg per mouse of recombinant mouse CXCL12 (rCXCL12) had a significantly delayed telogen-to-anagen transition compared with the control group. The rCXCL12-treated mice showed less anagen HFs in their H & E- stained skin tissues. rCXCL12 dramatically reduced the hair weight in a dose-dependent manner (Fig. 2A). In addition, the inhibitory effect of rCXCL12 on hair growth was evaluated in an organ culture using mouse vibrissae (Fig. 2B) and human HFs (Fig. 2C); a significant inhibition of hair growth was observed following incubation with rCXCL12. In addition, the ability of rCXCL12 to trigger catagen entrance in C_3H mice was investigated, and anagen HFs were considerably reduced in the rCXCL12-treated mouse compared with the control, the percentage of mouse skin in the anagen phase was lower in rCXCL12-treated mouse (Fig. 2D). According to prior research findings, STAT signaling has been implicated in the maintenance of telogen HFs [26]. Thus, mouse vibrissae follicles were treated with 100 ng/mL of rCXCL12 for 24 h, and the protein levels of p-STAT3 and p-STAT5 were significantly elevated in the DP and ORS region of mouse vibrissae follicles (Fig. 2E). STAT3 and STAT5 phosphorylation was also assessed in primary hDP and hORS cells, and rCXCL12 treatment induced both STAT3 and STAT5 phosphorylation in an immunofluorescence assay (Fig. S2; see Supporting Information). In summary, our data suggest that CXCL12 inhibits hair growth via the STAT signaling pathway.

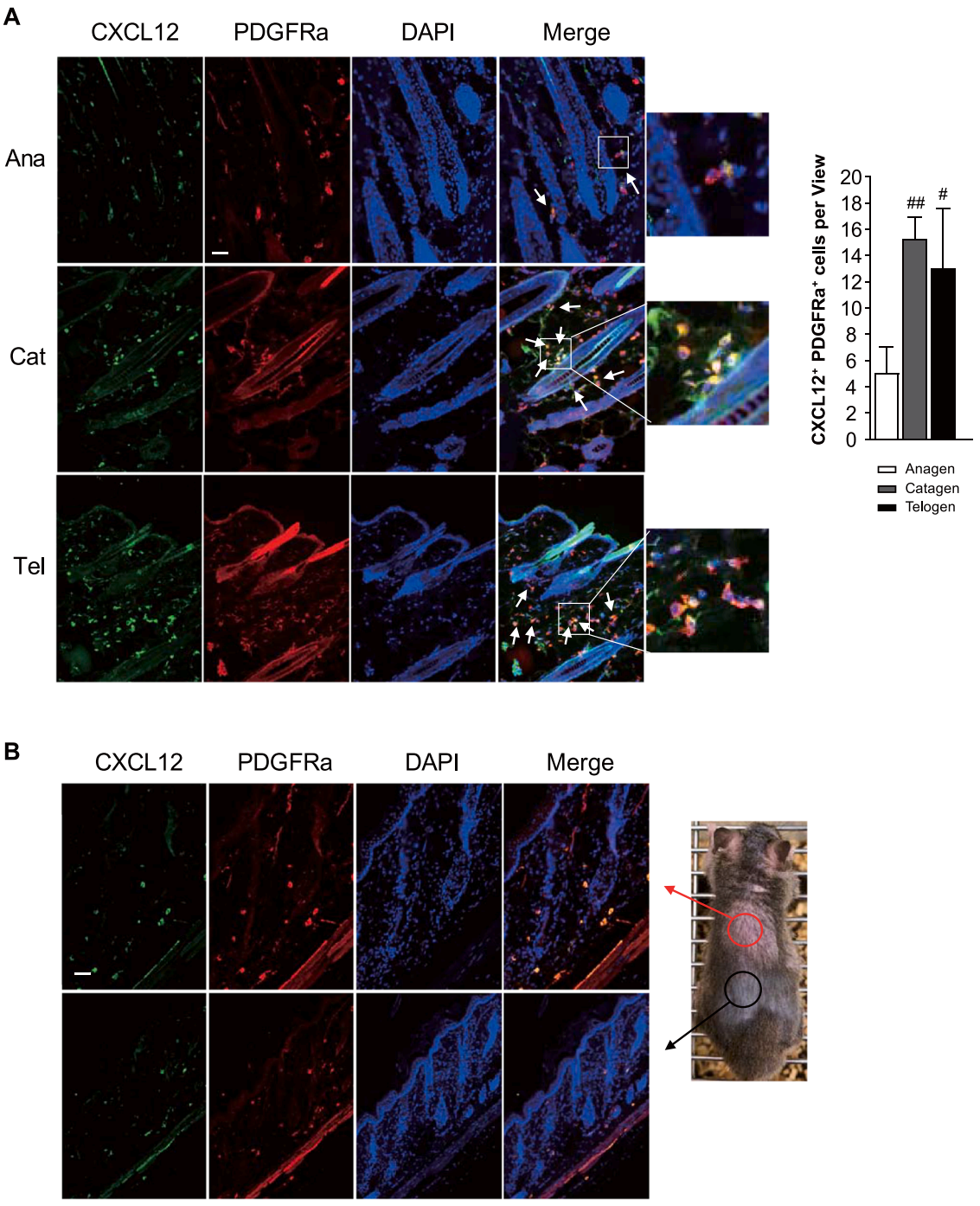

Fig. 1. Expression of CXCL12 in mouse and human hair follicles. (A) The paraffin sections were obtained using the back skin of 4-, 5-, and 7-week-old C_3H mice. CXCL12 (green) and PDGFRα (red, a dermal fibroblast marker) in mouse dorsal skin were detected by immunofluorescence. CXCL12 is costained with PDGFRα and primarily expressed in dermal fibroblasts. $CXCL12^+/PDGFR\alpha^+$ cells per view were counted (A, right panel) *# $p < 0.05$, ## $p < 0.01$* vs anagen phase. B) Bald (red arrow) and non-bald (black arrow) skin in the aged mice (>18 months) were harvested, and the expression of CXCL12 is increased in the balding region. DAPI staining (blue) indicates nuclei. Scale bar = 50 μm. (For interpretation of the references to color in this figure legend, the reader is referred to the web version of this article.)

3.3. Neutralization of CXCL12 promotes hair growth

To determine whether inhibiting CXCL12 could increase hair growth, 7-week-old C_3H mice were subcutaneously injected with an anti-CXCL12 neutralizing antibody (αCXCL12). In comparison with control treatment, mice treated with αCXCL12, at a dose of 25 μg each, had a significant increase in hair weight and anagen HF count (Fig. 3A). Further investigation of the effect of αCXCL12 on hair shaft growth was conducted using mouse vibrissae and human hair organ culture models. Individual HFs were isolated and cultured with vehicle control and αCXCL12 (Fig. 3B, C). αCXCL12 was found to considerably increase the length of mouse and human hair shafts. In addition, results of anagen elongation demonstrated that αCXCL12 delayed catagen phase induction in C_3H mice, and the percentage of mouse skin in the anagen phase was higher in the αCXCL12-treated mice (Fig. 3D). Confocal images showed that αCXCL12 treatment attenuated rCXCL12-induced p-STAT3 and p-STAT5 levels in hDP and hORS cells (Fig. S2; see Supporting Information).

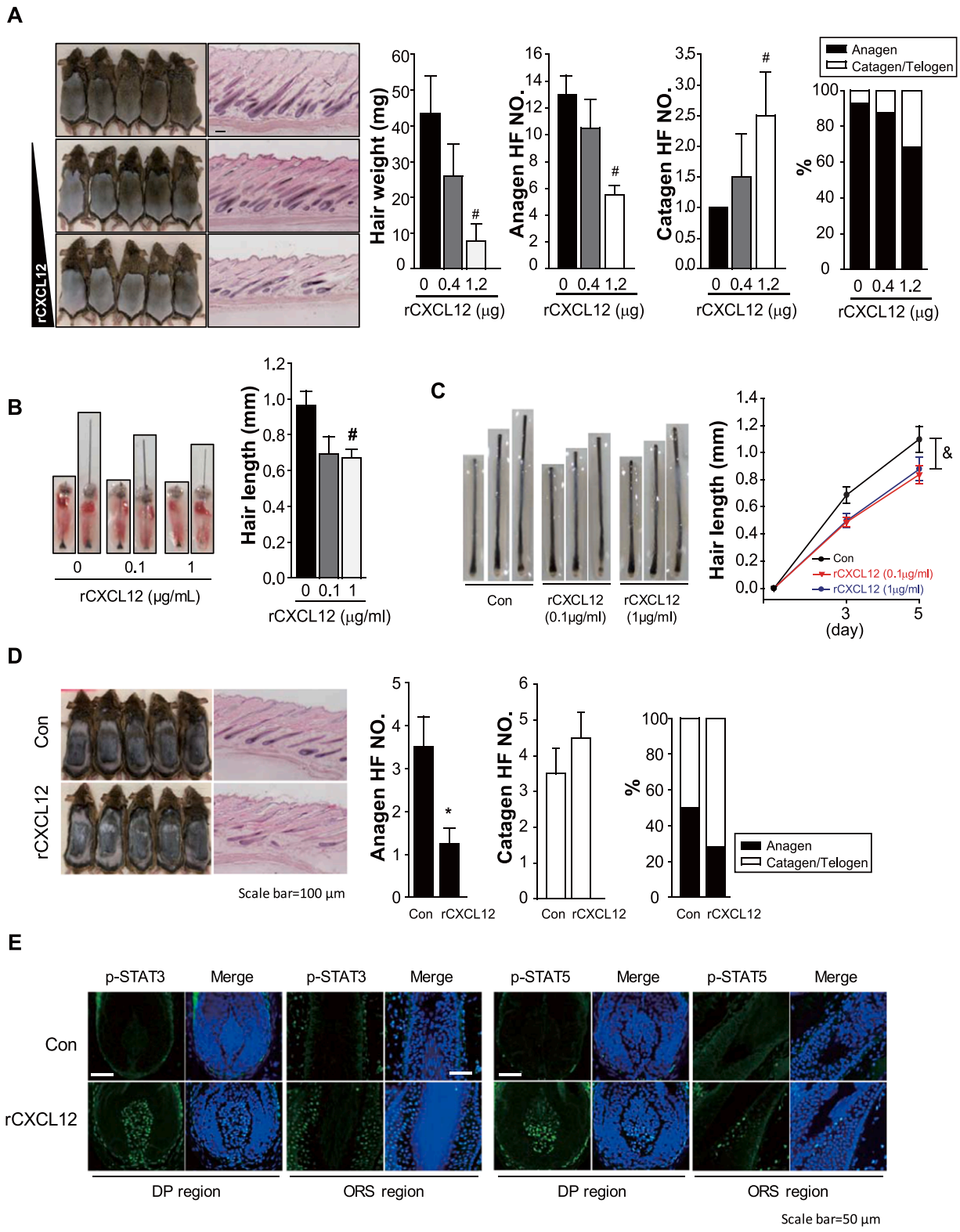

Fig. 2. Treatment of CXCL12 delays the entry of anagen and induces the entry of catagen. (A) The back skin of 7-week-old C_3H mice was shaved, and recombinant CXCL12 (rCXCL12) was subcutaneously injected. Compared with the negative control, subcutaneous injection of rCXCL12 delayed the telogen-to-anagen transition in C_3H mice on day 15. Hematoxylin and eosin (H&E)-staining was used to measure anagen HFs, catagen HFs, and the hair weight was compared. The percentage of anagen and non-anagen HFs was observed (right panel). # $p < 0.05$. Scale bar = 100 μm. (B, C) rCXCL12 treatment significantly inhibits the length of mouse vibrissa follicle (B) and human HFs (C). # $p < 0.05$, and & $p < 0.05$ vs con treated, n = 10–12 mouse vibrissa follicles per group, n = 10 human HFs per group. (D) In an anagen elongation experiment, anagen hair follicles were significantly reduced in rCXCL12 injected mice (as indicated by the arrow in H&E staining). Anagen HFs, catagen HFs, and the percentage of anagen and non-anagen HFs was observed (D, right panel). * $p < 0.05$, vs con treated. Scale bar = 100 μm. (E) p-STAT3 and p-STAT5 signals were analyzed via immunostaining after rCXCL12 incubation in vibrissae follicle, and STAT phosphorylation highly increased in the dermal papilla and outer root sheath of HF. Scale bar = 50 μm. Asterisk indicates a statistical difference in Student's t-test, sharp in one-way ANOVA with Tukey's post hoc test, and ampersand in two-way ANOVA with Tukey's Multiple Comparison Test.

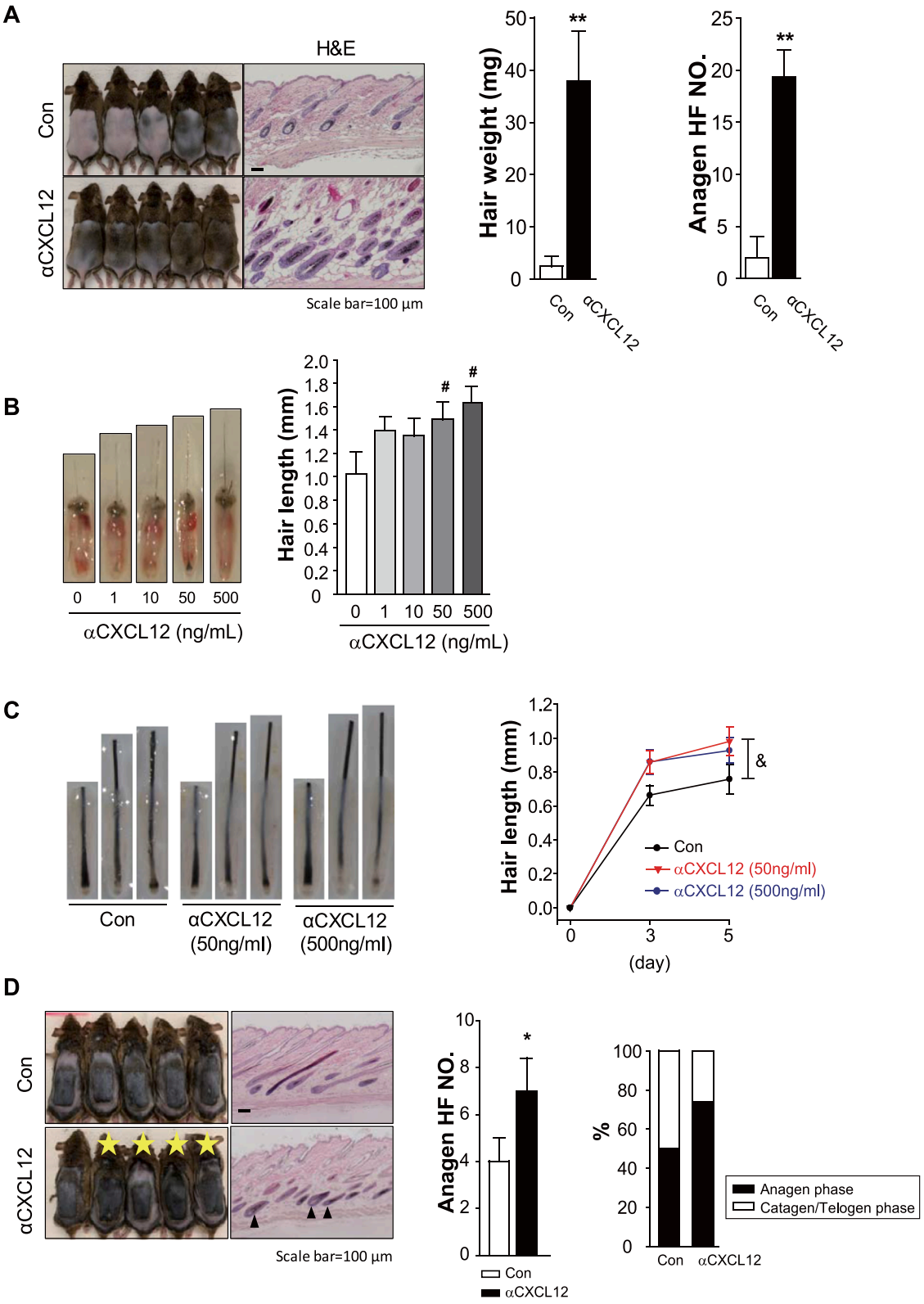

Fig. 3. Neutralization of CXCL12 promotes hair growth. (A) The back skin of 7-week-old C_3H mice was shaved, and neutralizing antibody for CXCL12 (αCXCL12) was subcutaneously injected. Compared with the negative control (IgG), αCXCL12 administration accelerated telogen-to-anagen transition in C_3H mice on day 15. H&E staining was used to measure anagen HFs, and the hair weight was compared. ** $p < 0.01$. Scale bar = 100 μm. (B, C) αCXCL12 significantly increased the length of mouse vibrissa follicles (B) and human hair follicles (HFs) (C). # $p < 0.05$ and & $p < 0.05$, vs con treated, n = 10–12 mouse vibrissa follicles per group, n = 10 human HFs per group. (D) In an anagen elongation experiment, anagen hair follicles were significantly increased in αCXCL12 injected mice (as indicated by the arrow in H&E staining). The percentage of anagen and non-anagen HFs was observed (D, right panel). * $p < 0.05$, vs con treated. Scale bar = 100 μm. Asterisk indicates statistical difference in Student's t-test, sharp in one-way ANOVA with Tukey's post hoc test, and ampersand in two-way ANOVA withTukey's Multiple Comparison Test.

3.4. CXCL12 knockdown by siRNA promotes hair growth

Further investigations were conducted to see whether CXCL12-targeting siRNA could aid hair growth. Human HFs were isolated and cultured with four si-CXCL12 and negative control, and si-CXCL12 was found to considerably increase hair length (Fig. 4A, left and middle). The reduced expression levels of CXCL12 were confirmed by qRT-PCR (Fig. 4A, right). Additionally, two si-CXCL12 enhanced the telogen-to-anagen transition in C_3H mice (Fig. 4B). The specificity of si-CXCL12 in mice was confirmed by immunofluorescence staining (Fig. S3, see Supporting Information). Simultaneously, the effect of si-CXCL12 on hair growth was also assessed using mouse vibrissae, and si-CXCL12 was found to increase hair length (Fig. 4C).

3.5. CXCR4 mediates hair cycle regulation of CXCL12

The expression of CXCL12 receptors, CXCR4 and CXCR7, was studied to have a better understanding about how CXCL12 acts on target cells in HFs. Confocal images showed that CXCR4 was expressed in DP (during anagen) and ORS cells of the mouse (Fig. 5A). CXCR4 was also detected in DP and ORS regions of human HFs (Fig. 5B). To determine whether suppressing CXCR4 or CXCR7 could increase hair growth, 7-week-old C_3H mice were subcutaneously injected with an anti-CXCR4 or anti-CXCR7 neutralizing antibody (αCXCR4/ αCXCR7). Compared with control IgG therapy, the mice injected with αCXCR4 at a dose of 25 μg each showed a substantial increase in hair weight (Fig. 5C), which αCXCR7 failed to do (Fig. S4; see Supporting Information). Furthermore, a CXCR4 receptor antagonist, plerixafor, considerably enhanced the telogen-to-anagen transition in animal model (Fig. 5D) and promoted the rCXCL12-induced inhibition of hair length in mouse vibrissa follicles (Fig. 5E). Confocal images showed that plerixafor treatment attenuated rCXCL12-induced p-STAT3 and p-STAT5 levels (Fig. S2; see Supporting Information). These findings suggest that CXCR4 contributes to CXCL12-mediated hair cycle control.

3.6. CXCL12 primarily expressed in DF, inhibits hair growth

To determine whether CXCL12 secreted by DFs mediates hair cycle regression, the secretion of CXCL12 by DFs was reduced using si-CXCL12 transfection. Mouse vibrissae, DPC, and ORS cells were then treated with DF conditioned medium (Fig. 6A). The si-CXCL12 transfection of DFs effectively reduced the CXCL12 level in the culture medium by approximately 90% compared with the control medium (Fig. 6B). We began by culturing mouse vibrissae follicles in conditioned medium from control cells ($DFCM^{Con\text{-}si}$) and si-CXCL12 transfected DF cells ($DFCM^{CXCL12\text{-}si}$). After two days of treatment with $DFCM^{CXCL12\text{-}si}$, the hair length of vibrissae follicles substantially increased (Fig. 6C). $DFCM^{CXCL12\text{-}si}$ treatment increased in DP cell proliferation and ALP1 mRNA level (Fig. 6D, and Fig. S5A; see Supporting Information). Furthermore, $DFCM^{CXCL12\text{-}si}$ treatment promoted ORS cell proliferation and migration (Fig. 6F, and Fig. S5B; see Supporting Information). These findings suggest that CXCL12 primarily expressed in DF, has an effect on DPCs and ORS in HFs, as well as control the hair cycle.

4. Discussion

This study aimed to determine where CXCL12 and CXCR4 are expressed in the vicinity of HFs and whether they limit hair growth. CXCL12 was shown to be highly expressed in DFs and elevated during the catagen and telogen stages of the hair cycle. In addition, CXCR4 is expressed in the dermal and epidermal layers of HFs. The rCXCL12 treatment caused hair loss, delaying the transition from telogen-to-anagen and reducing the hair length in hair organ culture. In hair organ culture, when CXCL12 was inhibited using a neutralizing antibody and siRNA, telogen-to-anagen transition was triggered, resulting in an increase in hair length. Furthermore, we investigated the molecular mechanisms and signaling pathways involved during the initial period of hair loss development. A neutralizing antibody and plerixafor dramatically increased hair growth by inhibiting CXCR4; however, CXCR7 neutralization had no effect on hair growth, and expression of CXCR7 during the hair cycle had no difference (Fig. S4; see Supporting Information). CXCL12 inhibition in DFs and treatment of conditioned media considerably increased hair length, and the proliferation of DPC and ORS cells in the hair organ culture. These findings suggest that DF-derived CXCL12 promotes hair loss by activating CXCR4 in HFs. CXCL12 and CXCR4 increased STAT3 and STAT5 phosphorylation in the dermal and epidermal layers of HFs. In contrast, a CXCL12-neutralizing antibody reduced the STAT3 and STAT5 signal in HFs. These findings indicate that CXCL12 primarily expressed in DFs inhibits hair growth via the CXCR4/STAT signaling pathway.

While CXCL12 and its receptors are widely expressed in the skin, their expression and functions during hair cycle progression have not been characterized. CXCL12, a stromal cell-derived factor widely expressed in DFs, activates CXCR4 to cause a variety of skin diseases, including hypertrophic scarring, keloid formation, psoriasis, and hyperpigmentation [27–29]. CXCL12 has a well-established role in hair graying. For instance, CXCL12 is highly expressed in the bulge region of human HFs and promotes melanocyte stem cell differentiation, a vital factor in preventing hair graying [30]. Moreover, CXCL12 and its receptor CXCR4 have been shown to control melanoblast migration and positioning during HF formation [17]. Of note, Sennett et al. found that early HF morphogenesis is not dependent on CXCR4 expression in the dermis or the epithelium of nascent HFs, although CXCR4 is transiently expressed in both these compartments [31]. In the present study, we demonstrated for the first time that CXCL12/CXCR4 pathway is involved in the hair cycle progression, DFs have high levels of CXCL12, and DF-derived CXCL12 impedes hair cycle progression by the inhibition of anagen and induction of catagen/telogen via activating CXCR4 in the ORS and DP of HFs.

CXCL12 is a chemokine that exhibits diverse functions via the Janus kinase (JAK)/ signal transducer and activator of transcription (STAT) pathway. For example, CXCL12 promots cancer cell proliferation and migration, making CXCL12 and CXCR4 potential anticancer drugs. CXCL12 inhibited cisplatin-induced apoptosis in human lung cancer cells by activating the JAK2/STAT3 signaling pathway [32]. CXCL12 induced STAT5 activation, which promoted proliferation in pre-B-ALL [33]. Determined by global gene expression analysis, inhibition of CXCL12 resulted in the downregulation of STAT3-related genes in leukemia stem cells [34]. Cancer cells can proliferate through the JAK/-STAT signaling pathway. However, activating the JAK/STAT pathway had varying impacts on hair growth and often caused hair loss. For instance, ruxolitinib and tofacitinib, which disrupt the JAK/STAT signaling pathway, have been shown to rapidly initiate anagen onset and subsequently result in hair growth [35]. In a phase III clinical trial, AA was reversed by the oral administration of inhibitors of the JAK/STAT pathways (e.g., ritrecitinib and baricitinib), which have been developed for use in patients with AA. In this study, CXCL12 therapy activated the STAT pathway, including STAT3 and STAT5 activation, in HFs, resulting in hair loss. However, silencing the CXCL12/CXCR4 pathway with siRNA and a neutralizing antibody inhibited STAT3 and STAT5 phosphorylation, thereby promoting hair growth. Therefore, it is plausible that CXCL12 causes hair loss via the JAK/STAT signaling pathway.

The role of CXCL families in AA is still debatable. Although CXCL9 and CXCL10 levels are elevated in the serum of AA patients, CXCL1 and CXCL12 levels are decreased [36]. A preliminary study found that CXCL12 expression increased in the HF of AA patients (data not shown), and lesional HFs, as previously reported [20]. Autologous γδ T cells promoted the collapse of HF immune privilege via CXCL12, and resident human dermal γδ T cells served as stress sentinels [21]. However, CXCL isoforms, such as CXCL9, CXCL10, CXCL11, and their receptor CXCR3, have been shown to contribute to the pathogenesis of AA [37]. The overexpression of CXCL12 and other inflammatory and immune

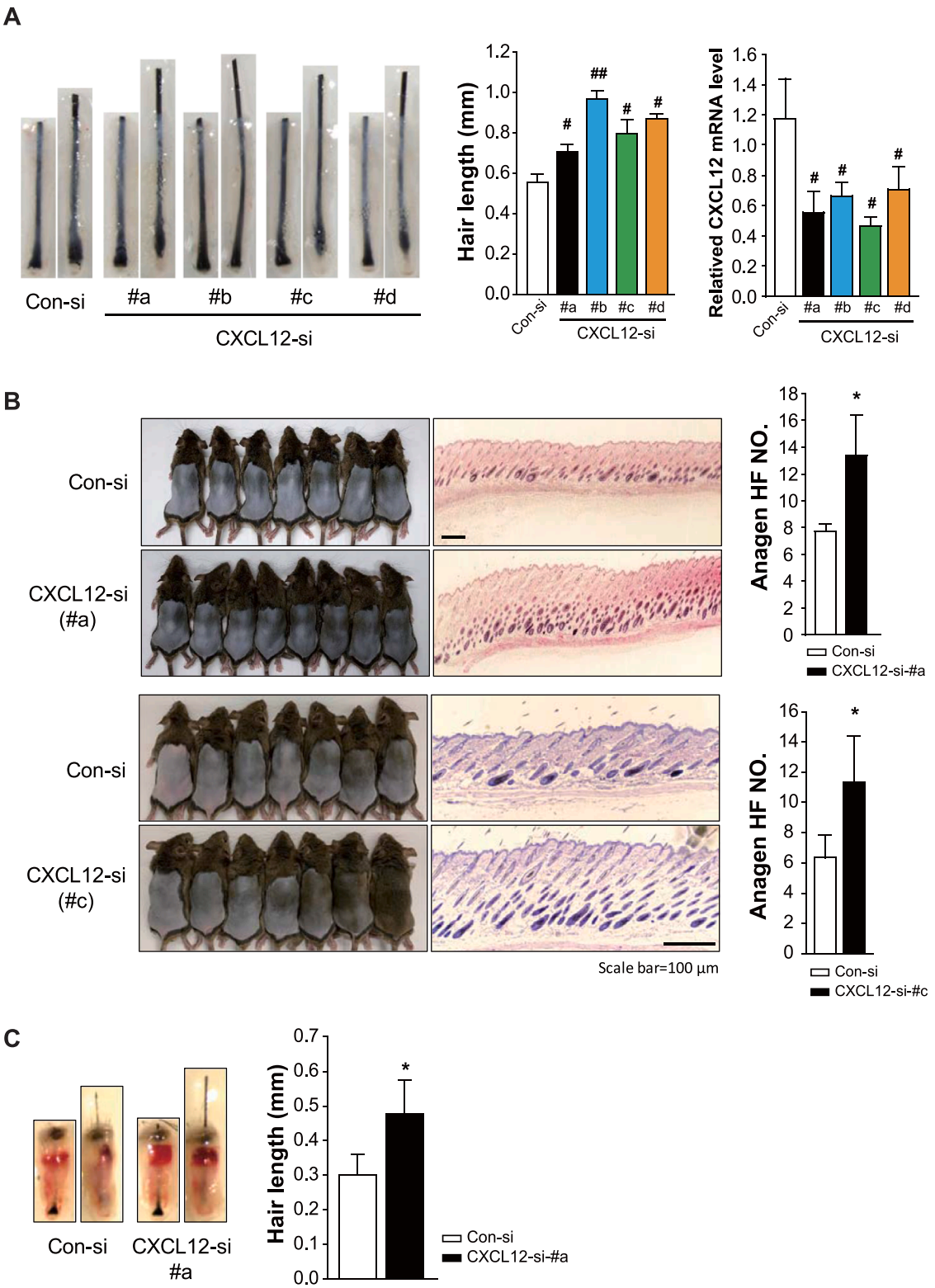

Fig. 4. CXCL12 knockdown by siRNA promotes hair growth. (A) Human hair follicles were isolated and cultured with multiple species of CXCL12-si (#a, #b, #c, and #d) treatment (1 μg) for 4 days. Images of HFs were taken on day 0 & day 4 with a stereomicroscope. CXCL12 knockdown increased hair fiber length in the organ culture. The expression of CXCL12 under different conditions was confirmed by qRT-PCR. # $p < 0.05$; ## $p < 0.01$, vs con-si treated, n = 10 HFs per group. (B) After depilating of the dorsal skin, 6 μg of CXCL12-si-#a or CXCL12-si-#c was injected subcutaneously every 2 days. Injection of siRNA for CXCL12 accelerated the telogen-to-anagen transition in C_3H mice. Scale bar = 100 μm. (C) Mouse vibrissa follicles were isolated and cultured with CXCL12-si-#a treatment (1 μg) for 2 days, and CXCL12 knockdown increased hair fiber length. * $p < 0.05$, vs con-si treated, n = 10–12 mouse vibrissa follicles per group. Asterisk indicates statistical difference in Student's t-test, and sharp in one-way ANOVA.

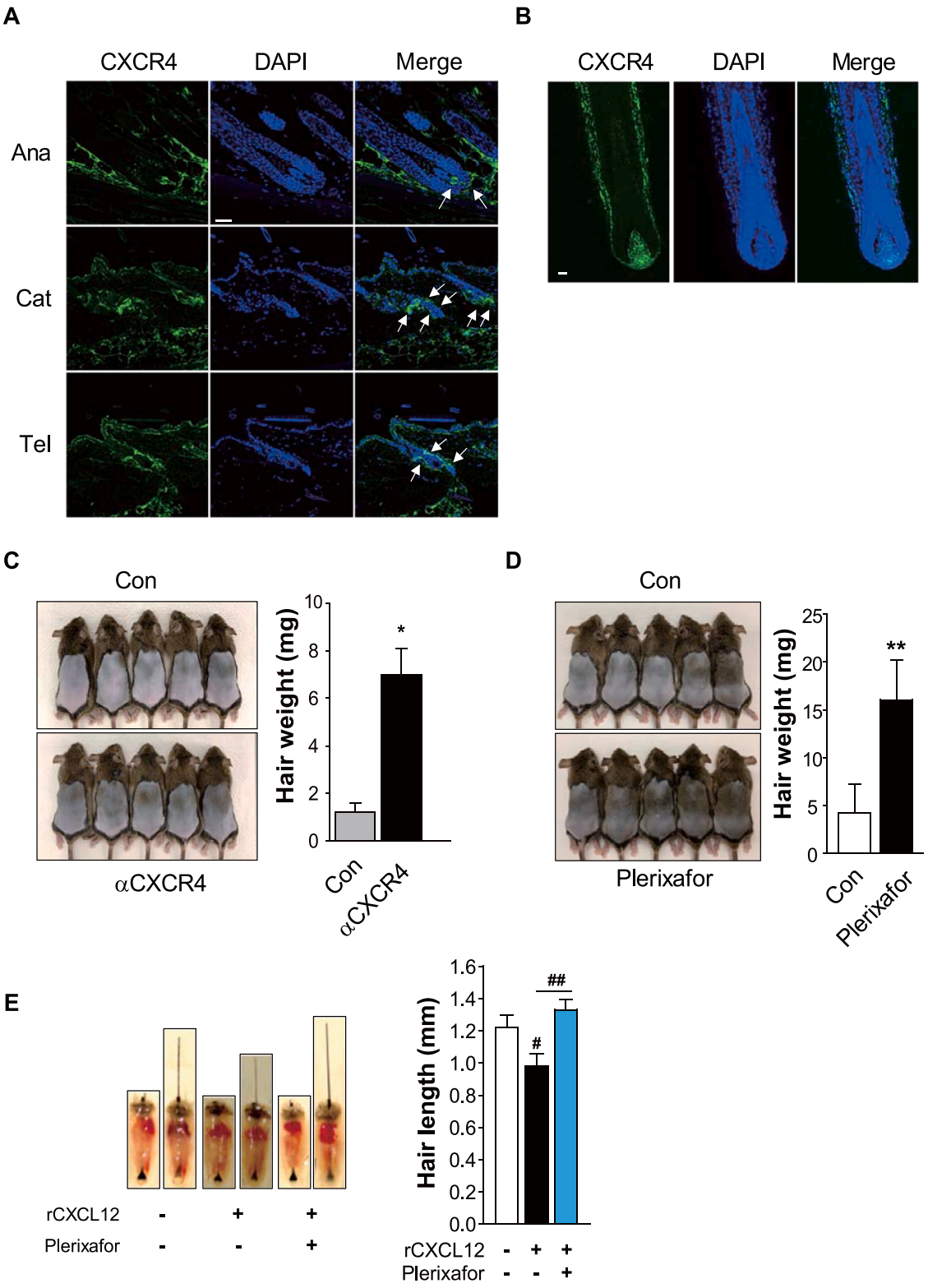

Fig. 5. CXCR4 mediates hair cycle regulation of CXCL12. (A) The paraffin sections were obtained using the dorsal skin of 4-, 5-, and 7-week-old C_3H mice. Detection of CXCR4 (green) in mice using immunofluorescence showed that it is expressed in the epidermal and dermal layers of hair follicles. (B) Immunostaining showed that CXCL12 is expressed in DP and ORS regions of human HFs. (C) Neutralizing antibody for CXCR4 (αCXCR4) was subcutaneously injected into 7-week-old C_3H mice. Compared with the negative control, αCXCR4 administration facilitated telogen-to-anagen transition, and the hair weight increased. (D) CXCR4 antagonist (Plerixafor, AdooQ, USA) treatment also promoted telogen-to-anagen transition. * $p < 0.05$, ** $p < 0.01$. (E) Plerixafor increased the rCXCL12-induced inhibition of hair length in mouse vibrissa follicles. * $p < 0.05$, vs con-treated; ## $p < 0.01$, vs rCXCL12-treated group, n = 10–12 mouse vibrissa follicles per group. Scale bar = 50 μm.(For interpretation of the references to color in this figure legend, the reader is referred to the web version of this article.)

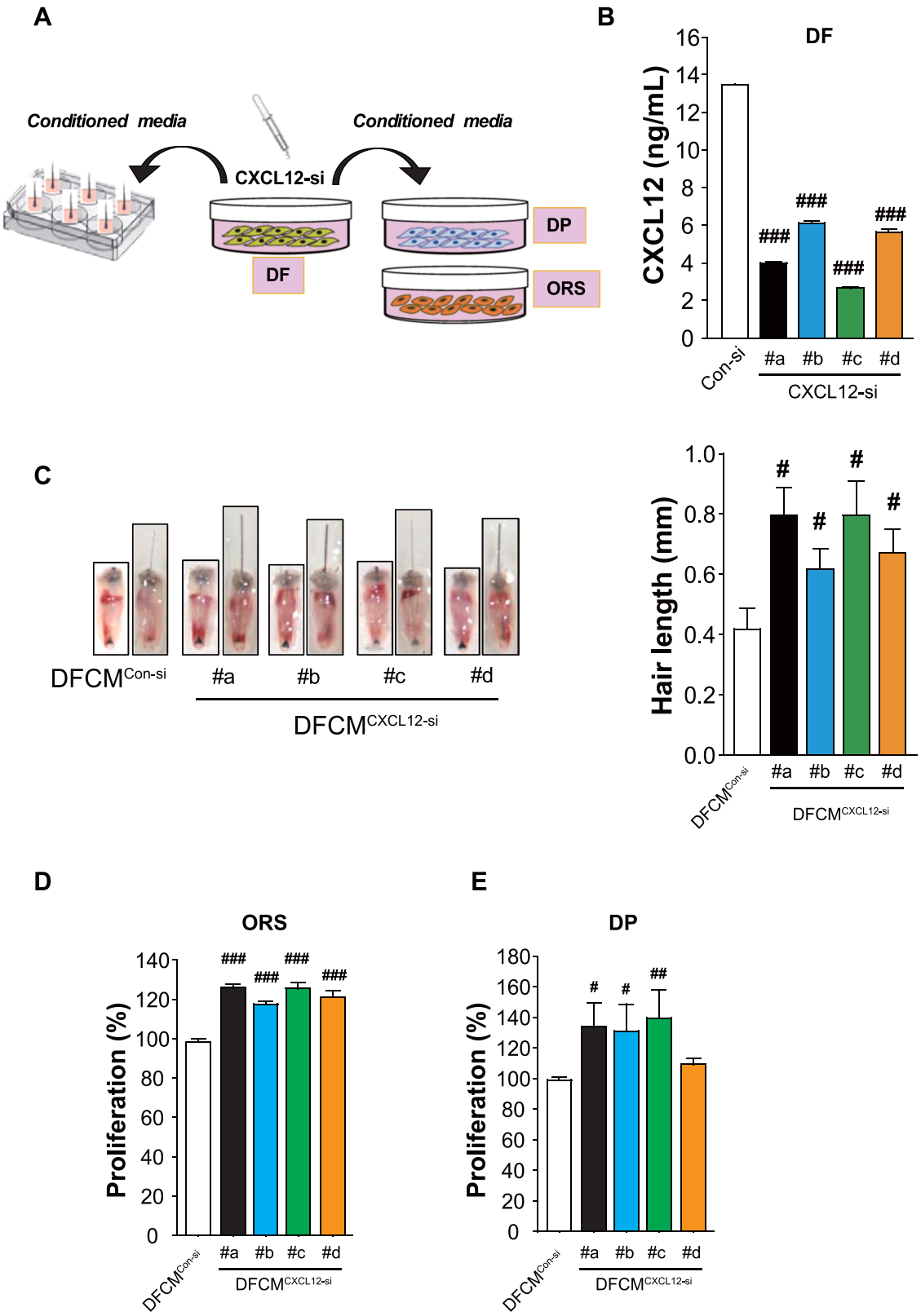

Fig. 6. CXCL12 secreted from dermal fibroblasts inhibits hair growth. The experimental design. After transfecting si-CXCL12 in DF cells for 6 h, the culture medium was replaced with fresh media, and then the cells were incubated for another 48 h to collect the culture medium ($DFCM^{con\text{-}si}$ & $DFCM^{CXCL12\text{-}si}$). (B) The concentration of CXCL12 under different conditions was significantly decreased in $DFCM^{CXCL12\text{-}si}$. (C) $DFCM^{CXCL12\text{-}si}$ treatment increased hair fiber length in the mouse vibrissae organ culture. *# $p < 0.05$,* vs con-treated, n = 10–12 mouse vibrissa follicles per group. (D, E) $DFCM^{CXCL12\text{-}si}$ treatment increased the proliferation of hDPCs (D) and ORS cells, *# $p < 0.05$; ## $p < 0.01$, ### $p < 0.001$* vs con-treated. Sharp indicates a statistical difference in one-way ANOVA.

mediators in AA patients, suggests that neutralizing CXCL12 or inhibiting CXCR4 in the AA microenvironment may be effective in its treatment. Thus, CXCL12 inhibition may be a novel therapeutic approach for AA, which we intend to investigate in future studies.

Author contributions

M.Z., S.H.O., and **J.H.S.** were involved in the study conception and design. **M.Z.** made a significant contribution to all the experiments. **M.Z., N.C.**, and **Y.J.C** were involved in the acquisition of data. **M.Z., N.C., Y.J.C.**, and **J.H.S.** analyzed and interpreted the data. **M.Z.** and **J.H.S.** prepared the manuscript. **S.H.O.** and **J.K.** provided human hair follicle samples. All authors reviewed the manuscript.

Conflict of interest statement

The authors have declared that no competing interest exists.

Acknowledgements

This research was supported by the Korean Government and the Tech Incubator Program for Startup Korea (Grant no. 10388970) and by the Korea Drug Development Fund funded by the Ministry of Science and ICT, Ministry of Trade, Industry, and Energy, and Ministry of Health and Welfare (HN22C0027, Republic of Korea).

Appendix A. Supporting information

Supplementary data associated with this article can be found in the online version at doi:10.1016/j.biopha.2022.112996.

References

[1] G.C. Beck, B.A. Yard, A.J. Breedijk, K. Van Ackern, F.J. Van Der Woude, Release of CXC-chemokines by human lung microvascular endothelial cells (LMVEC) compared with macrovascular umbilical vein endothelial cells, Clin. Exp. Immunol. 118 (2) (1999) 298–303.
[2] Y. Han, T. He, D.R. Huang, C.A. Pardo, R.M. Ransohoff, TNF-alpha mediates SDF-1 alpha-induced NF-kappa B activation and cytotoxic effects in primary astrocytes, J. Clin. Investig. 108 (3) (2001) 425–435.
[3] D.M. Durrant, B.P. Daniels, R.S. Klein, IL-1R1 signaling regulates CXCL12-mediated T cell localization and fate within the central nervous system during West Nile Virus encephalitis, J. Immunol. 193 (8) (2014) 4095–4106.
[4] C. Britton, M.C. Poznansky, P. Reeves, Polyfunctionality of the CXCR4/CXCL12 axis in health and disease: implications for therapeutic interventions in cancer and immune-mediated diseases, FASEB J. 35 (4) (2021), e21260.
[5] K. Golan, O. Kollet, T. Lapidot, Dynamic cross talk between S1P and CXCL12 regulates hematopoietic stem cells migration, development and bone remodeling, Pharmaceuticals 6 (9) (2013) 1145–1169.
[6] J.M. Burns, B.C. Summers, Y. Wang, A. Melikian, R. Berahovich, Z. Miao, M. E. Penfold, M.J. Sunshine, D.R. Littman, C.J. Kuo, K. Wei, B.E. McMaster, K. Wright, M.C. Howard, T.J. Schall, A novel chemokine receptor for SDF-1 and I-TAC involved in cell survival, cell adhesion, and tumor development, J. Exp. Med. 203 (9) (2006) 2201–2213.
[7] K. Balabanian, B. Lagane, S. Infantino, K.Y. Chow, J. Harriague, B. Moepps, F. Arenzana-Seisdedos, M. Thelen, F. Bachelerie, The chemokine SDF-1/CXCL12 binds to and signals through the orphan receptor RDC1 in T lymphocytes, J. Biol. Chem. 280 (42) (2005) 35760–35766.
[8] Q. Ma, D. Jones, P.R. Borghesani, R.A. Segal, T. Nagasawa, T. Kishimoto, R. T. Bronson, T.A. Springer, Impaired B-lymphopoiesis, myelopoiesis, and derailed cerebellar neuron migration in CXCR4- and SDF-1-deficient mice, Proc. Natl. Acad. Sci. USA 95 (16) (1998) 9448–9453.
[9] T. Nagasawa, K. Tachibana, T. Kishimoto, A novel CXC chemokine PBSF/SDF-1 and its receptor CXCR4: their functions in development, hematopoiesis and HIV infection, Semin Immunol. 10 (3) (1998) 179–185.
[10] B. Li, W. Bai, P. Sun, B. Zhou, B. Hu, J. Ying, The effect of CXCL12 on endothelial progenitor cells: potential target for angiogenesis in intracerebral hemorrhage, J. Interferon Cytokine Res. 35 (1) (2015) 23–31.
[11] A. Neesse, V. Ellenrieder, NEMO-CXCL12/CXCR4 axis: a novel vantage point for antifibrotic therapies in chronic pancreatitis? Gut 66 (2) (2017) 211–212.
[12] T. Liu, X. Li, S. You, S.S. Bhuyan, L. Dong, Effectiveness of AMD3100 in treatment of leukemia and solid tumors: from original discovery to use in current clinical practice, Exp. Hematol. Oncol. 5 (2015) 19.
[13] J.S. Song, C.C. Chang, C.H. Wu, T.K. Dinh, J.J. Jan, K.W. Huang, M.C. Chou, T. Y. Shiue, K.C. Yeh, Y.Y. Ke, T.K. Yeh, Y.N. Ta, C.J. Lee, J.K. Huang, Y.C. Sung, K. S. Shia, Y. Chen, A highly selective and potent CXCR4 antagonist for hepatocellular carcinoma treatment, Proc. Natl. Acad. Sci. USA 118 (13) (2021).
[14] I.G. Winkler, A.R. Pettit, L.J. Raggatt, R.N. Jacobsen, C.E. Forristal, V. Barbier, B. Nowlan, A. Cisterne, L.J. Bendall, N.A. Sims, J.P. Levesque, Hematopoietic stem cell mobilizing agents G-CSF, cyclophosphamide or AMD3100 have distinct mechanisms of action on bone marrow HSC niches and bone formation, Leukemia 26 (7) (2012) 1594–1601.
[15] L. Chen, Q. Zhang, Q.H. Chen, F.Y. Ran, L.M. Yu, X. Liu, Q. Fu, G.Y. Song, J. M. Tang, T. Zhang, Combination of G-CSF and AMD3100 improves the anti-inflammatory effect of mesenchymal stem cells on inducing M2 polarization of macrophages through NF-kappaB-IL1RA signaling pathway, Front Pharmacol. 10 (2019) 579.
[16] F. Di Giacomo, D. Lewandowski, E. Cabannes, V. Nancy-Portebois, M. Petitou, S. Fichelson, P.H. Romeo, Heparan sulfate mimetics can efficiently mobilize long-term hematopoietic stem cells, Haematologica 97 (4) (2012) 491–499.
[17] A. Belmadani, H. Jung, D. Ren, R.J. Miller, The chemokine SDF-1/CXCL12 regulates the migration of melanocyte progenitors in mouse hair follicles, Differentiation 77 (4) (2009) 395–411.
[18] E. Lee, J. Han, K. Kim, H. Choi, E.G. Cho, T.R. Lee, CXCR7 mediates SDF1-induced melanocyte migration, Pigment Cell Melanoma Res. 26 (1) (2013) 58–66.
[19] L. Michel, P. Reygagne, P. Benech, F. Jean-Louis, S. Scalvino, S. Ly Ka So, Z. Hamidou, S. Bianovici, J. Pouch, B. Ducos, M. Bonnet, A. Bensussan, A. Patatian, E. Lati, J. Wdzieczak-Bakala, J.C. Choulot, E. Loing, M. Hocquaux, Study of gene expression alteration in male androgenetic alopecia: evidence of predominant molecular signalling pathways, Br. J. Dermatol. 177 (5) (2017) 1322–1336.
[20] Y. Uchida, J. Gherardini, A. Schulte-Mecklenbeck, M. Alam, J. Cheret, A. Rossi, T. Kanekura, C.C. Gross, A. Arakawa, A. Gilhar, M. Bertolini, R. Paus, Pro-inflammatory Vdelta1(+)T-cells infiltrates are present in and around the hair bulbs of non-lesional and lesional alopecia areata hair follicles, J. Dermatol. Sci. 100 (2) (2020) 129–138.
[21] Y. Uchida, J. Gherardini, K. Pappelbaum, J. Cheret, A. Schulte-Mecklenbeck, C. C. Gross, N. Strbo, A. Gilhar, A. Rossi, W. Funk, T. Kanekura, L. Almeida, M. Bertolini, R. Paus, Resident human dermal gammadeltaT-cells operate as stress-sentinels: Lessons from the hair follicle, J. Autoimmun. 124 (2021), 102711.
[22] R. Paus, N. Ito, M. Takigawa, T. Ito, The hair follicle and immune privilege, J. Investig. Dermatol. Symp. Proc. 8 (2) (2003) 188–194.
[23] T. Jindo, R. Imai, K. Takamori, H. Ogawa, Organ culture of mouse vibrissal hair follicles in serum-free medium, J. Dermatol. 20 (12) (1993) 756–762.
[24] J. Hye Kim, S. Gyu Park, W.K. Kim, S.U. Song, J.H. Sung, Functional regulation of adipose-derived stem cells by PDGF-D, Stem Cells 33 (2) (2015) 542–556.
[25] R. Paus, K.S. Stenn, R.E. Link, Telogen skin contains an inhibitor of hair growth, Br. J. Dermatol. 122 (6) (1990) 777–784.
[26] J.M.D. Legrand, E. Roy, J.J. Ellis, M. Francois, A.J. Brooks, K. Khosrotehrani, STAT5 activation in the dermal papilla is important for hair follicle growth phase induction, J. Investig. Dermatol. 136 (9) (2016) 1781–1791.
[27] Z. Chen, Z. Gao, L. Xia, X. Wang, L. Lu, X. Wu, Dysregulation of DPP4-CXCL12 Balance by TGF-beta1/SMAD pathway promotes CXCR4(+) inflammatory cell infiltration in keloid scars, J. Inflamm. Res 14 (2021) 4169–4180.
[28] N.H. Abdelaal, N.G. Elhefnawy, S.R. Abdulmonem, S. Sayed, N.A. Saleh, M. A. Saleh, Evaluation of the expression of the stromal cell-derived factor-1 alpha (CXCL 12) in psoriatic patients after treatment with Methotrexate, J. Cosmet. Dermatol. 19 (1) (2020) 253–258.
[29] J.E. Yoon, Y. Kim, S. Kwon, M. Kim, Y.H. Kim, J.H. Kim, T.J. Park, H.Y. Kang, Senescent fibroblasts drive ageing pigmentation: a potential therapeutic target for senile lentigo, Theranostics 8 (17) (2018) 4620–4632.
[30] T. Yamada, S. Hasegawa, Y. Hasebe, M. Kawagishi-Hotta, M. Arima, Y. Iwata, T. Kobayashi, S. Numata, N. Yamamoto, S. Nakata, K. Sugiura, H. Akamatsu, CXCL12 regulates differentiation of human immature melanocyte precursors as well as their migration, Arch. Dermatol. Res. 311 (1) (2019) 55–62.
[31] R. Sennett, A. Rezza, K.L. Dauber, C. Clavel, M. Rendl, Cxcr4 is transiently expressed in both epithelial and mesenchymal compartments of nascent hair follicles but is not required for follicle formation, Exp. Dermatol. 23 (10) (2014) 748–750.
[32] M. Wang, T. Lin, Y. Wang, S. Gao, Z. Yang, X. Hong, G. Chen, CXCL12 suppresses cisplatin-induced apoptosis through activation of JAK2/STAT3 signaling in human non-small-cell lung cancer cells, Oncol. Targets Ther. 10 (2017) 3215–3224.
[33] F. Mowafi, A. Cagigi, L. Matskova, O. Bjork, F. Chiodi, A. Nilsson, Chemokine CXCL12 enhances proliferation in pre-B-ALL via STAT5 activation, Pediatr. Blood Cancer 50 (4) (2008) 812–817.
[34] P. Agarwal, S. Isringhausen, H. Li, A.J. Paterson, J. He, A. Gomariz, T. Nagasawa, C. Nombela-Arrieta, R. Bhatia, Mesenchymal niche-specific expression of Cxcl12 controls quiescence of treatment-resistant leukemia stem cells, Cell Stem Cell 26 (1) (2020) 123.
[35] S. Harel, C.A. Higgins, J.E. Cerise, Z. Dai, J.C. Chen, R. Clynes, A.M. Christiano, Pharmacologic inhibition of JAK-STAT signaling promotes hair growth, Sci. Adv. 1 (9) (2015), e1500973.
[36] N. Zainodini, G. Hassanshahi, M.K. Arababadi, H. Khorramdelazad, A. Mirzaei, Differential expression of CXCL1, CXCL9, CXCL10 and CXCL12 chemokines in alopecia areata, Iran. J. Immunol. 10 (1) (2013) 40–46.
[37] Z. Dai, L. Xing, J. Cerise, E.H. Wang, A. Jabbari, A. de Jong, L. Petukhova, A. M. Christiano, R. Clynes, CXCR3 blockade inhibits T cell migration into the skin and prevents development of alopecia areata, J. Immunol. 197 (4) (2016) 1089–1099.